

Delta-doped AlGaN/GaN metal–oxide–semiconductor heterostructure field-effect transistors with high breakdown voltages

Z. Y. Fan, J. Li, J. Y. Lin, and H. X. Jiang

Citation: [Applied Physics Letters](#) **81**, 4649 (2002); doi: 10.1063/1.1527984

View online: <http://dx.doi.org/10.1063/1.1527984>

View Table of Contents: <http://scitation.aip.org/content/aip/journal/apl/81/24?ver=pdfcov>

Published by the [AIP Publishing](#)

Articles you may be interested in

[AlGaN/GaN polarization-doped field-effect transistor for microwave power applications](#)

Appl. Phys. Lett. **84**, 1591 (2004); 10.1063/1.1652254

[Gate leakage effects and breakdown voltage in metalorganic vapor phase epitaxy AlGaN/GaN heterostructure field-effect transistors](#)

Appl. Phys. Lett. **80**, 3207 (2002); 10.1063/1.1473701

[Mechanism of radio-frequency current collapse in GaN–AlGaN field-effect transistors](#)

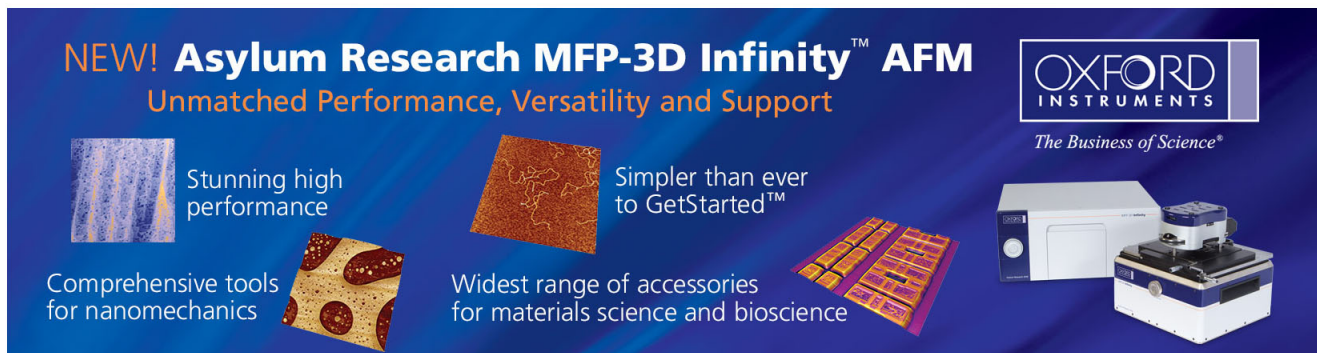
Appl. Phys. Lett. **78**, 2169 (2001); 10.1063/1.1363694

[AlGaN/GaN metal–oxide–semiconductor heterostructure field-effect transistors on SiC substrates](#)

Appl. Phys. Lett. **77**, 1339 (2000); 10.1063/1.1290269

[Analysis of Schottky gate electron tunneling in polarization induced AlGaN/GaN high electron mobility transistors](#)

J. Appl. Phys. **86**, 3398 (1999); 10.1063/1.371240



NEW! Asylum Research MFP-3D Infinity™ AFM
Unmatched Performance, Versatility and Support

OXFORD INSTRUMENTS
The Business of Science®

Stunning high performance
Simpler than ever to GetStarted™
Comprehensive tools for nanomechanics
Widest range of accessories for materials science and bioscience

The advertisement features four images: a blue textured surface, a brown textured surface, a grid of colorful rectangular samples, and the MFP-3D Infinity AFM instrument itself.

Delta-doped AlGaN/GaN metal–oxide–semiconductor heterostructure field-effect transistors with high breakdown voltages

Z. Y. Fan, J. Li, J. Y. Lin, and H. X. Jiang^{a)}

Department of Physics, Kansas State University, Manhattan, Kansas 66506-2601

(Received 15 July 2002; accepted 16 October 2002)

The fabrication and dc characteristics of AlGaN/GaN-based heterostructure field-effect transistors (HFETs) by employing the δ -doped barrier and the SiO₂ insulated gate are reported. The device grown on sapphire substrate has a high drain-current-driving and gate-control capabilities as well as a very high gate-drain breakdown voltage of 200 V for a gate length of 1 μ m and a source-drain distance of 3 μ m. The incorporation of the SiO₂ insulated gate and the δ -doped barrier into HFET structures reduces the gate leakage and improves the two-dimensional channel carrier mobility, and thereby allows one to take the inherent advantage of AlGaN/GaN HFETs with relatively high Al contents—the device structure is capable to deliver higher electron density (or drain current density) yet ensures an excellent pinch-off property as well as small gate leakage current. These characteristics indicate a great potential of this structure for high-power-microwave applications.

© 2002 American Institute of Physics. [DOI: 10.1063/1.1527984]

AlGaN/GaN heterostructure field-effect transistors (HFETs) have attracted considerable attentions in the past decade for applications in the area of high power and high temperature microwave electronics due to the unique properties of III-nitrides, including wide band gaps, high electron saturation velocities, and high critical breakdown fields.^{1,2} Considerable progress has been made to improve the nitride HFET power and voltage handling abilities.^{3,4} However, it has been observed that the Schottky gate of HFET tends to degrade with enhanced gate leakage current and insufficient pinch-off characteristics, especially when the HFETs are operating under high power conditions. The degradation of the gate leads to the premature breakdown and, hence, a deficient device performance with a reduction of output power, the rf efficiency and noise figure.⁵ It is believed that the premature breakdown is caused by the traditional gate-drain diode breakdown as a result of the thermionic emission,⁶ or the thermal effect as a consequence of the surface hopping conduction of gate leakage current.⁷ Different gate insulation layers, such as SiO₂,^{8,9} Si₃N₄,^{10,11} Ga₂O₃,^{12,13} and AlN¹⁴ have been employed as one of the possible solutions to tackle the gate leakage problem by increasing the energy barrier. It has been demonstrated that a thin SiO₂ or AlN layer under the gate dramatically reduced the gate leakage current by several orders.^{9,14} Another advantage of adopting the insulation layer was thought that it has the effect to reduce the electrical field in the underlying nitride semiconductor and, hence, increase the gate breakdown voltage.¹⁵

To further reduce the current tunneling through the low quality deposited thin gate oxide layer and, hence, increase the gate-drain breakdown voltage, here we propose to replace the uniformly doping scheme in the AlGaN barrier with a δ -doping profile. With the dopants farther away from the gate, the gate leakage current would be reduced. Moreover, with an optimized separation distance between the dop-

ants and the AlGaN/GaN interface, carrier-impurity scattering can be minimized and, hence, carrier mobility would be enhanced. Comparing with uniformly doped HFET structures, the δ -doping profile is also likely to reduce trapping effect and improve threshold voltage control as well as breakdown characteristics. These advantages have been demonstrated in the GaAs and InP based HFETs structures.^{16,17}

Figure 1 shows a schematic diagram of the metal–oxide–semiconductor HFET (MOSHFET) layer structure used in this study. The AlGaN/GaN heterostructures were grown by metalorganic chemical vapor deposition on sapphire substrates. Following a 50 nm GaN nucleation layer on the substrate, a 1 μ m highly resistive GaN layer was deposited. A very thin AlN interfacial layer (\sim 1 nm) was subsequently deposited above GaN to separate the channel from the AlGaN barrier layer and to improve the sheet charge density and mobility by increasing the confinement of electrons in the channel and decreasing the alloy scattering.^{18,19}

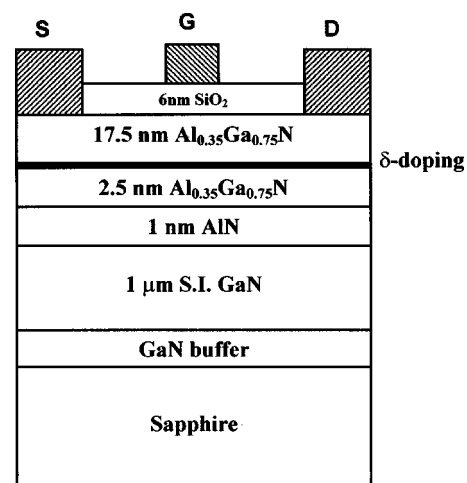


FIG. 1. The schematic diagram of the Si δ -doped AlGaN/GaN MOSHFET layer structure. The device has a gate length (L_g) of 1 μ m, gate width (W_g) of $2 \times 40 \mu$ m for a double gate or 80 μ m for a single gate, and a source-drain distance (L_{sd}) of 3 μ m.

^{a)}Electronic mail: jjiang@phys.ksu.edu

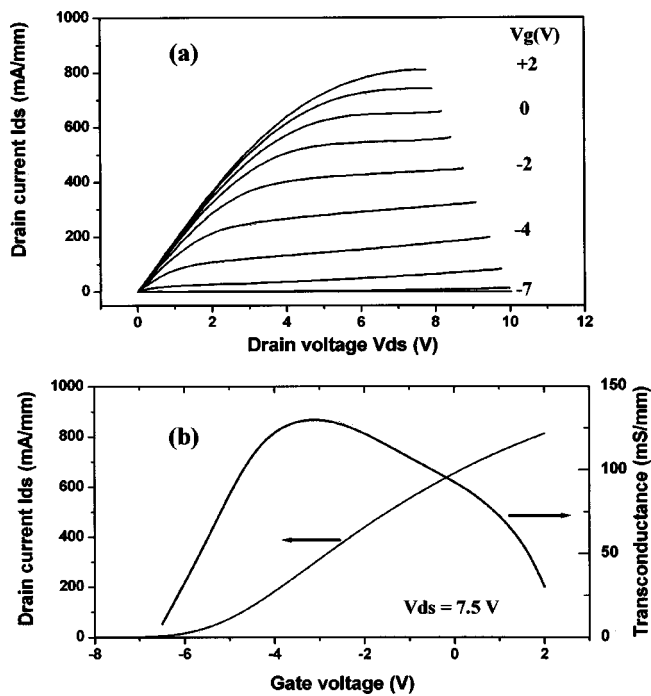


FIG. 2. (a) dc I - V characteristics and (b) transfer characteristics for a $1 \times 80 \mu\text{m} \times 1 \mu\text{m}$ AlGaIn/GaN MOSHFET with δ -doped barrier. In (a) the gate was biased from 2 to -7 V in a step of -1 V, in (b) the drain bias was 7.5 V. A maximum drain saturation current of 0.82 A/mm, a peak extrinsic transconductance of 130 mS/mm, and a threshold voltage of -7 V were achieved.

The heterostructure was then capped by a Si δ -doped $\text{Al}_{0.35}\text{Ga}_{0.65}\text{N}$ barrier layer with a thickness of 20 nm, grown at 1050°C . A δ -junction-like Si doping profile was implemented by interrupting the usual crystal-growth mode by closing the Ga (trimethylgallium) and Al (trimethylaluminum) flows, while the Si impurities (SiH_4) were introduced into the growth chamber. The δ -doping profile was verified by secondary ion mass spectroscopy measurement (performed by Charles and Evan) for a selective sample. The device fabrication started from the mesa isolation performed by chlorine-based inductively coupled plasma etching. The high resistivity of the GaN layer ensured the electrical isolation between devices with an etch depth of ~ 250 nm. The ohmic metal stack of Ti (20 nm)/Al (150 nm)/Ti (30 nm)/Au (50 nm) was deposited by an electron-beam evaporator, and followed by lift-off, ohmic contacts were formed by rapid thermal annealing of the sample in nitrogen atmosphere at 850°C for 30 s. A 6-nm-thick SiO_2 layer and gate metal stack of Ni/Au were then deposited to form an insulated gate. The device has a gate length (L_g) of $1 \mu\text{m}$, gate width (W_g) of $2 \times 40 \mu\text{m}$ for a double gate or $80 \mu\text{m}$ for a single gate, and a source-drain distance (L_{sd}) of $3 \mu\text{m}$.

Figure 2(a) shows the on-wafer measured drain-source dc I - V characteristics of a MOSHFET device with a δ -doped $\text{Al}_{0.35}\text{Ga}_{0.65}\text{N}$ barrier, and the related dc transfer characteristics are shown in Fig. 2(b). The original δ -doped $\text{Al}_{0.35}\text{Ga}_{0.65}\text{N}/\text{GaN}$ HFET structure exhibited an electron mobility and sheet carrier density of about $1330 \text{ cm}^2/\text{Vs}$ and 1.34×10^{13} , respectively, as obtained by Hall measurement. The fabricated device exhibits a high drain current driving ability and excellent pinch-off property. The drain current arrives a maximum value of ~ 0.82 A/mm at a gate bias of 2

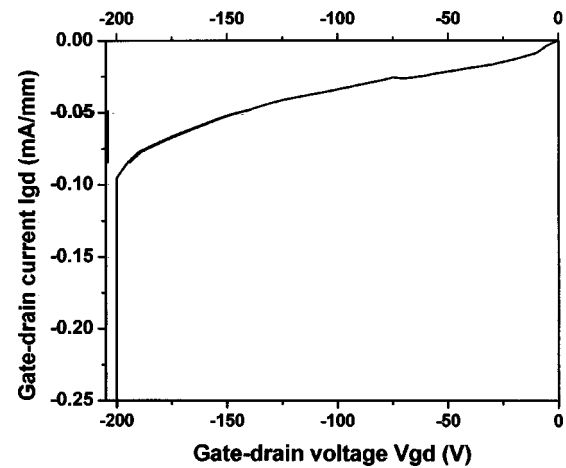


FIG. 3. The gate leakage current I_{gd} vs gate-drain voltage V_{gd} of an AlGaIn/GaN MOSHFET with δ -doped AlGaIn barrier. A very high gate-drain breakdown voltage (~ 200 V) was obtained.

V and a drain bias of 8 V, which is among the better values reported for devices grown on sapphire substrate. The slightly larger knee voltage (6 V) could be attributed to the δ -doping scheme in the $\text{Al}_{0.35}\text{Ga}_{0.65}\text{N}$ barrier, because the source and the drain were directly formed on the undoped $\text{Al}_{0.3}\text{Ga}_{0.7}\text{N}$ without recessing etch, leading to a larger contact resistance. The device was completely pinched off at a gate bias of -7 V. In this off state, the drain current was less than 0.5 mA/mm at a drain bias of 8 V, implying a ratio exceeding 10^3 for the on/off state current control capability. A peak extrinsic transconductance g_m of 130 mS/mm was achieved at a gate bias of -3 V. The measured transconductance profile was quite broad which is expected to provide a large gate voltage swing as well as dynamic range for power and linearity.¹⁰ The performance was much improved over that of a uniformly doped HFET with a similar current density that was found to be difficult to pinch off due to its much higher leakage current.

Pulsed I - V characteristics were also measured to observe the dispersion (or trapping effect) between I - V characteristics under dc and ac gate drives. Any dispersion would directly reduce the output power and efficiency under ac operation. Comparing the I - V characteristics obtained under dc and pulsed ($80 \mu\text{s}$) gate drives, no significant dispersion was observed in the δ -doped MOSHFET for drain voltages up to 30 V, demonstrating the rf dispersion was not serious in these devices at low voltages, a major improvement over those of uniformly doped devices. However, after the device was stressed under high voltages exceeding 100 V, a 30%–40% reduction in the maximum drain current was observed, implying further improvements are still needed.

The power performance of the device depends on the maximum drain voltage before breakdown sets in. Since our devices incorporated SiO_2 insulation layer under the gate and a δ -doping scheme, we expect the gate leakage current to be much reduced and the gate breakdown voltage to be increased. Indeed, this is demonstrated in Fig. 3. A very high gate-drain breakdown voltage of ~ 200 V was achieved in our MOSHFET with a $1 \mu\text{m}$ gate length and a source-drain distance of $3 \mu\text{m}$. Beyond pinch-off with a gate bias of -8 V, a drain-source breakdown voltage of ~ 180 V was also observed.

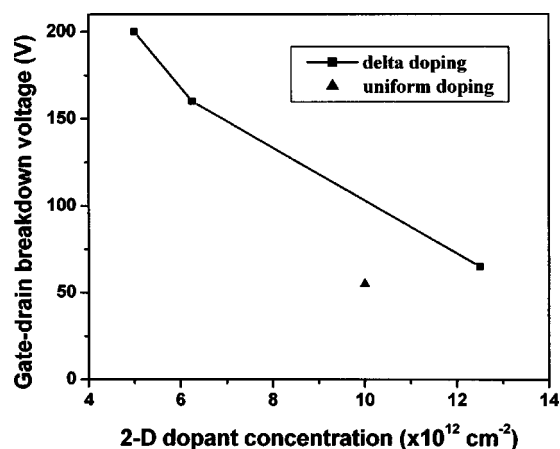


FIG. 4. The gate-drain breakdown voltage vs the Si-dopant concentration for MOSHFET devices with δ -doped AlGaIn barriers. The breakdown voltage for one of the MOSHFETs with uniformly doped AlGaIn barrier is also shown for comparison. At a comparable doping level, the δ -doped MOSHFET structure exhibits a much higher breakdown voltage than the uniformly doped device.

It is expected that the doping level as well as the doping profile in the HFET structure, which determines the gate electron emission or tunneling current, plays an important role in the nitride HFET breakdown. MOSHFETs were fabricated in the same batch from δ -doped HFET structures with different Si dopant concentrations as well as from uniformly doped structures. The δ -doped HFET structures exhibited electron mobilities and sheet carrier densities ranging from 1330 to 1160 cm^2/Vs and from 1.34×10^{13} to $1.55 \times 10^{13} \text{ cm}^{-2}$, respectively, as the effective Si dopant concentration in the δ -doped plane varied from $5 \times 10^{12} \text{ cm}^{-2}$ to $1.25 \times 10^{13} \text{ cm}^{-2}$. Figure 4 compares the gate-drain breakdown voltages of these devices. As we can see, for the δ -doping scheme, the gate-drain breakdown voltage was reduced from 200 to 65 V as the effective Si dopant concentration was increased from $5 \times 10^{12} \text{ cm}^{-2}$ to $1.25 \times 10^{13} \text{ cm}^{-2}$. At higher sheet densities, electrons may spill over from the two-dimensional channel into the barrier region, which would enhance the gate leakage current and thereby decrease the breakdown voltage between the drain and the gate. Included in Fig. 4 is also the breakdown voltage of one device fabricated from a uniformly doped $\text{Al}_{0.35}\text{Ga}_{0.65}\text{N}/\text{GaN}$ HFET structure with an effective Si dopant concentration of about $1 \times 10^{13} \text{ cm}^{-2}$. It can be seen that at this dopant concentration the uniformly doped device withstands a much lower breakdown voltage (~ 60 V) than a value of 100 V for the δ -doped device, demonstrating the advantage of the δ -doping scheme over uniform doping.

In summary, we have fabricated AlGaIn/GaN based MOSHFETs with high drain-current-driving and gate-control

capabilities, and a very high gate-drain breakdown voltage of 200 V for a 1 μm gate length and a source-drain distance of 3 μm . The improved characteristics were obtained by incorporating insulating gate oxide and δ -doped AlGaIn barrier layers. Our unique device structure by combining the SiO_2 insulated gate and the δ -doped barrier allowed us to take the inherent advantage of AlGaIn/GaN HFETs with relatively high Al contents—the device structure delivers high channel electron densities (or equivalently high drain current density), while it also ensures an excellent pinch-off property, small gate leakage current, and hence, a reduced degradation of the gate performance. These characteristics indicate a great potential of this structure for high power microwave applications.

This research is supported by BMDO (Dr. Kepi Wu), monitored by USASMDC (Dr. Fred Clarke and Terry Bauer) and DOE (DE-FG03-96ER45604). The authors wish to thank W. P. Zhao for the lithography work and S. X. Jin for help in device fabrication.

- ¹T. P. Chow and R. Tyagi, IEEE Trans. Electron Devices **41**, 1481 (1994).
- ²M. Asif Khan, Q. Chen, J. W. Yang, M. S. Shur, B. T. Dermott, and J. A. Higgins, IEEE Electron Device Lett. **17**, 325 (1996).
- ³S. T. Sheppard, K. Doverspike, W. L. Pribble, S. T. Allen, J. W. Palmour, L. T. Kehias, and T. J. Jenkins, IEEE Electron Device Lett. **20**, 161 (1999).
- ⁴Y.-F. Wu, D. Kapolnek, J. P. Ibbetson, P. Parikh, B. P. Keller, and U. K. Mishra, IEEE Trans. Electron Devices **48**, 586 (2001).
- ⁵N. Maeda, T. Saitoh, K. Tsubaki, T. Nishida, and N. Kobayash, Jpn. J. Appl. Phys., Part 2 **38**, L987 (1999).
- ⁶E. Alekseev, P. Nguyen-Tan, D. Pavlidis, M. Micovic, D. Wong, and C. Nguyen, Proc. 17th IEEE/Cornell Conf., Ithaca, NY, August 2000, p. 84.
- ⁷W. S. Tan, P. A. Houston, P. J. Parbrook, D. A. Wood, G. Hill, and C. R. Whitehouse, Appl. Phys. Lett. **80**, 3207 (2002).
- ⁸M. Asif Khan, X. Hu, G. Sumin, A. Lunev, J. Yang, R. Gaska, and M. S. Shur, IEEE Electron Device Lett. **21**, 63 (2000).
- ⁹M. Asif Khan, X. Hu, A. Tarakji, G. Simin, J. Yang, R. Gaska, and M. S. Shur, Appl. Phys. Lett. **77**, 1339 (2000).
- ¹⁰E. M. Chumbes, J. A. Smart, T. Prunty, and J. R. Shealy, IEEE Trans. Electron Devices **48**, 416 (2001).
- ¹¹X. Hu, A. Koudymov, G. Simin, J. Yang, M. Asif Khan, A. Tarakji, M. S. Shur, and R. Gaska, Appl. Phys. Lett. **79**, 2832 (2001).
- ¹²F. Ren, M. Hong, S. N. G. Chu, M. A. Marcus, M. J. Schurman, A. Baca, S. J. Pearton, and C. R. Abernathy, Appl. Phys. Lett. **73**, 3893 (1998).
- ¹³K. Inoue, Y. Ikeda, H. Masato, T. Matsuno, and K. Nishii, IEDM, 2001.
- ¹⁴D. H. Cho, M. Shimizu, T. Ide, H. Ookita, and H. Okumura, Jpn. J. Appl. Phys., Part 1 **41**, 4481 (2002).
- ¹⁵B. Gaffey, L. J. Guido, X. W. Wang, and T. P. Ma, IEEE Trans. Electron Devices **48**, 458 (2001).
- ¹⁶H. Hida, K. Ohata, Y. Suzuki, and H. Toyoshima, IEEE Trans. Electron Devices **33**, 601 (1986).
- ¹⁷K. W. Kim, H. Tiang, and M. A. Littlejohn, IEEE Trans. Electron Devices **38**, 1737 (1991).
- ¹⁸L. Hsu and W. Walukiewicz, J. Appl. Phys. **89**, 1783 (2001).
- ¹⁹L. Shen, S. Heikman, B. Moran, R. Coffie, N.-Q. Zhang, D. Buttari, I. P. Smorchkova, S. Keller, S. P. DenBaars, and U. K. Mishra, IEEE Electron Device Lett. **22**, 457 (2001).